HYDRODYNAMICS OF TIDAL FLOW ACROSS A SUBMARINE SAND RIDGE: LESSONS FROM MIDDLE GROUND

Tess Brandon

MITSG 07-21

Hydrodynamics of Tidal Flow Across A Submarine Sand Ridge
Lessons from Middle Ground

Tess Brandon
Summer Student Fellow
Woods Hole Oceanographic Institution
31 August 2007

Advised by:
Al Plueddemann, PO
Rich Signell, USGS
Rocky Geyer, AOP&E

I. Abstract

Middle Ground is a sand ridge that runs along the channel of Vineyard Sound just west of West Chop headland on Martha's Vineyard. The ridge is situated in the channel at a slight angle to reversing tidal flow along the channel. This tidal flow is asymmetrical with respect to the ridge, with the ebb cycle stronger to the north of the ridge and the opposite true on the south side, resulting in a counterclockwise mean flow around the ridge. The goal of this study was to resolve the small-scale processes on and around the ridge that are responsible for its maintenance and shape. This was done by collection and analysis of *in situ* water velocity measurements and comparison of the data to a numerical model. Harmonic analysis was performed on a moored ADCP time series, which confirmed the ebb dominance on the north side of the ridge. A mean flow of 5-10 cm/s was found to flow in the direction of the ebb tide and was confirmed by the model. In order to extend the *in situ* observations to locations closer to the ridge, spatial transects across the ridge were obtained using the Autonomous Underwater Vehicle REMUS over a complete tidal cycle. Analysis of REMUS data showed a strong localized shearing of velocity over the ridge crest during the strongest currents. Comparison to the model indicated some spatial variability in the tidal asymmetry relative to the ridge. More field observations from both mooring and REMUS data are necessary to fully resolve the small-scale processes most relevant to Middle Ground.

Outline

II. Introduction

Middle Ground, a submarine sand ridge in Vineyard Sound, is located just to the west of the northern-most headland on Martha's Vineyard. The orientation of this headland, called West Chop, is nearly normal to the direction of the tidal currents (Figure 1). The geography of this region can be used to explain the presence of Middle Ground. As the ebb tide flows past the headland, it transports sediment. Once west of the headland, frictional shearing along the coast of Martha's Vineyard causes the flow to turn. In turning it loses momentum and deposits sediment just to the west of West Chop. As the ebb cycle progresses, the sediment pile grows and elongates along the axis of the channel. During the flood cycle, flow along the west coast of Martha's Vineyard pushes the pile back northward along the axis of the channel. The result is a net accumulation of sediment in the area of Middle Ground over the tidal cycle (Signell & Harris, 2000).

Figure 1: Location of Middle Ground relative to West Chop on Martha's Vineyard, and direction of tidal flow in the area.

This process explains the existence of Middle Ground. The ridge was first described in detail in 1969, and does not appear to have changed significantly in that time. Thus, the objective of this project is to gain an understanding of the small-scale processes that are responsible for maintaining and shaping the ridge over time. With a combination of theory, field measurements and a model, we attempt to complete the story of Middle Ground.

III. Background

Middle Ground

The geomorphology of Middle Ground was first described by Smith. It is a submarine sand ridge of 10-12 kilometers in length, with a sharp crest at approximately 5 meters depth. The

major axis of the ridge runs approximately east-west, with a sharp termination at the western end. The ridge is also characterized by sets of sand waves, with one set on the north side of the ridge and one on the south (Smith 1969). These sand waves have a wavelength of 100-200 meters, and are migrating with the tide towards the ridge at a rate of several centimeters a day. The United States Geological Survey (USGS) performed three swath bathymetry surveys covering the western end of Middle Ground in the fall of 2006 and May of 2007. Figure 2 shows the image generated from the May survey. The region covered by the survey includes the region in which we collected field measurements for this project.
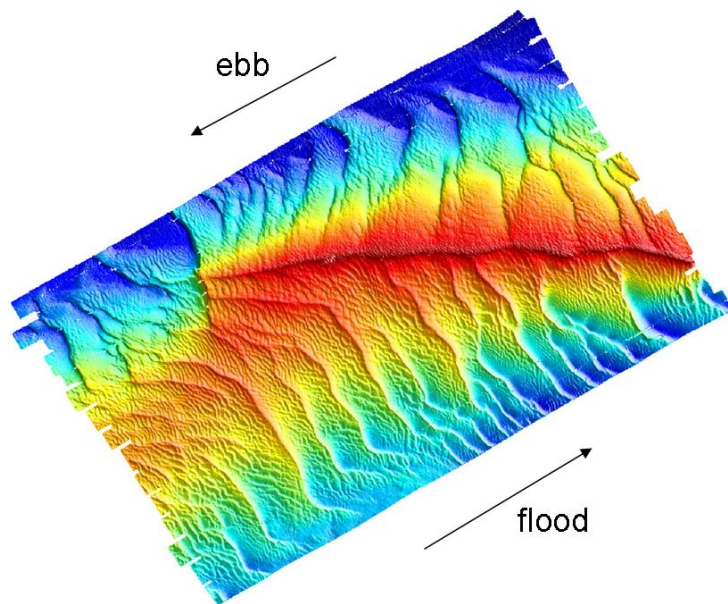

Figure 2: Results of USGS swath bathymetry survey, May 2007. This figure also shows the directions of the ebb and flood tides in this region.

The tides in Vineyard Sound are highly rectilinear and dominated by M2, with the principal tidal ellipse axis oriented along the sound. The tidal amplitude is asymmetrical with respect to the ridge. On the north side of Middle Ground, the ebb tide is stronger than the flood tide, and on the south side of the ridge the opposite is true. This is consistent with the geography of the headland forcing previously discussed, as well as with the direction of sand wave migration (see Figure 2). This asymmetry results in a tidal residual flow that circulates counterclockwise around Middle Ground.

Regional Oceanic Modeling System

The Regional Oceanic Modeling System (ROMS) has been used to model tides in many different regions. For the purpose of this project, we use ROMS in Vineyard Sound. In the region surrounding Middle Ground the model has an average resolution of 100-120 meters per pixel. ROMS uses bathymetry and tidal information to output water velocity information over the entire water column. The bathymetry in ROMS is a smoothed representation of bathymetry from standard NOAA bathymetric charts. An example of information output by ROMS is shown in Figure 3.
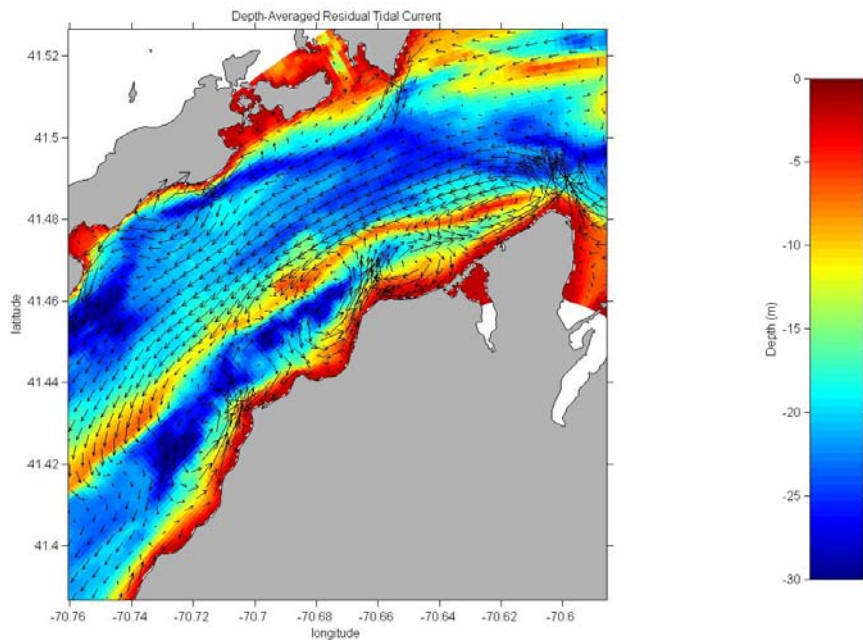
Figure 3: Example of output from ROMS in Vineyard Sound. Arrows represent tidal residual flow. Color is indicative of bathymetry, with Middle Ground visible as the thin red line running down the south half of the channel.

As mentioned, the goal of this project was to resolve the small-scale processes that deal with tidal flow on and around Middle Ground. We compared ROMS against our field measurements in order to test the ability of the model to predict and describe these small-scale processes. If the model succeeded with a high degree of accuracy, we might use it to gain information on areas and processes difficult to measure *in situ*.

Small-scale Processes

Several models in the literature address questions very similar to the questions we pose about Middle Ground. Each describes a set of forces or a process that results in a ridge situated, as Middle Ground is, oblique to reversing tidal flow. It is likely that none of these small-scale processes is solely responsible for the maintenance and shaping of Middle Ground. However, by understanding how each of these models relates to Middle Ground, we can interpret our field observations in a relevant context. Thus we can begin to create a more complete story of Middle Ground. The following provides an overview of four of the small-scale processes described in the literature that are most relevant to Middle Ground.

a. Tidal Residual Flow

As described by Smith and confirmed by ROMS, the asymmetry of the tide relative to Middle Ground results in a tidal residual circulation around the ridge. This residual may work in two ways to shape and maintain Middle Ground. First, it causes the migration of the sand waves on either side towards the ridge, providing a mechanism for sediment to accumulate on the ridge.

Second, the direction of flow around the ridge may result in a net convergence of water, and thus sediment, towards the center of the circulation path. This idea is consistent with the large-scale headland effect discussed in the previous section.

b. Stirring the Teacup

Pingree (1978) described how reversing tidal flow across headlands can result in sediment convergence and the creation of sand banks. His model, or the "stirring-the-teacup" theory, focuses on residual eddy formation on either side of the headland as a result of "tidal stirring." These eddies are mirror images of each other across the ridge. Thus, one eddy is clockwise, and the other counterclockwise, forcing a residual current directly offshore of the headland. Pingree states that sediment will accumulate in the low pressure center of these eddies if the tidal stirring of the eddy overtakes Earth's rotation. Thus, sediment is more likely to accumulate in the center of a counterclockwise eddy in the Northern Hemisphere (Figure 4).
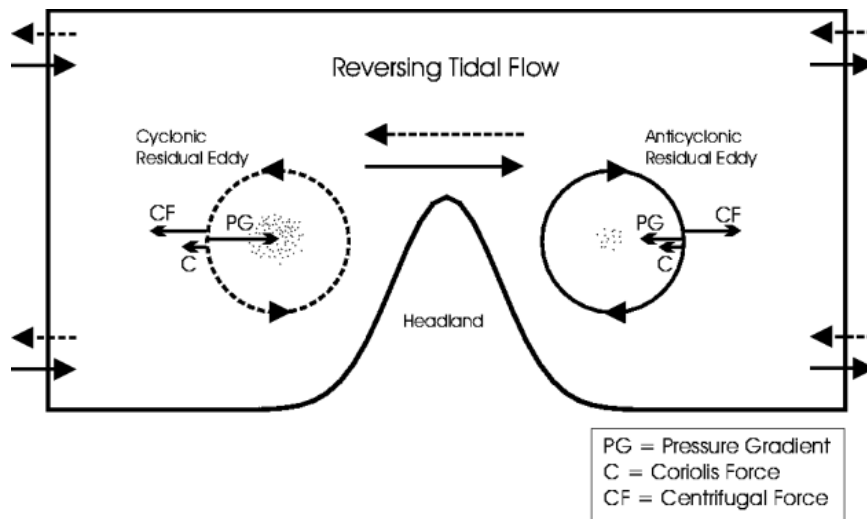

Figure 4: Forces in balance to generate an accumulation of sediment. Diagram modified from Pingree (1978) by Signell & Harris (2000).

As previously discussed, the tidal asymmetry in Vineyard Sound relative to Middle Ground results in a counterclockwise circulation around the ridge. If we consider this residual circulation to be a tidal eddy, we may use Pingree's model to explain the continuous accumulation of sand to maintain Middle Ground.

c. Bottom Friction

Where Pingree and Smith describe the residual circulation around the ridge to be a direct result of the tidal asymmetry, Huthnance (1973) proposes another mechanism that may be responsible for, or contribute to, the tidal asymmetry itself. Consider the southern side of Middle Ground. During the flood tide, as a uniform tidal flow moves obliquely onto the ridge, the increase in bottom friction as a result of shallower water causes the flow to slow until it the frictional and pressure gradient forces are once again balanced. During the ebb tide, as the tidal flow moves off the ridge into deeper water, the effect of bottom friction is reduced. Thus the flow gains speed until the pressure gradient is again balanced by friction. As shown by Figure 5, over the

tidal cycle this has the effect of a mean flow parallel to the ridge in the eastward direction. Applying this model to the opposite side of the ridge, the result is opposing net flow parallel to Middle Ground. This net flow would contribute to the tidal flow and result in an apparent asymmetry in the flood and ebb tides relative to the ridge. In the case of Middle Ground, the ebb tide would be stronger to the north and the flood stronger to the south. This is indeed what Smith described.
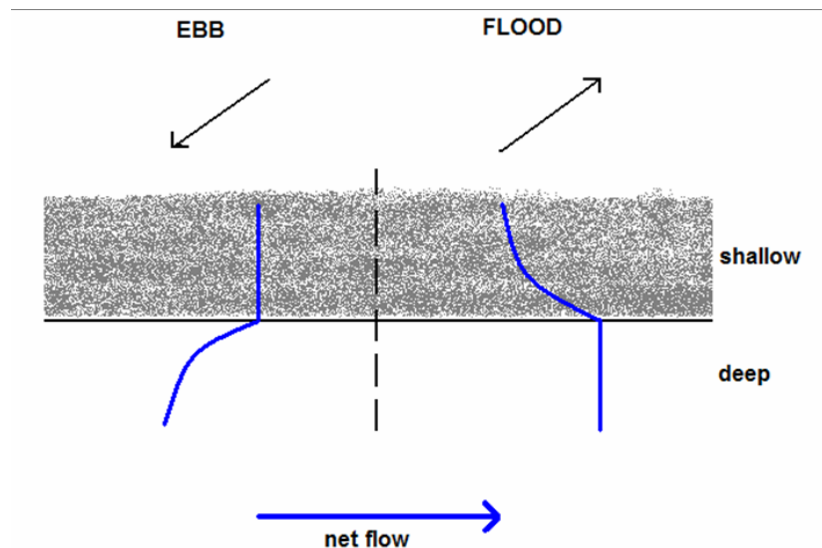

Figure 5: The effect of bottom friction on the south side of a sand ridge. Modified from Huthance (1973).

d. Vorticity Change Over A Sand Bank

Robinson (1983) discusses circulation around parallel sandbanks oriented obliquely against reversing tidal flow. Middle Ground runs approximately parallel to the coastline of Martha's Vineyard; thus this discussion is relevant. Expanding on Huthance's two-dimensional analysis of this situation, Robinson focuses on the vorticity mechanisms which operate when residual flows run parallel to a sandbar. As tidal flow moves obliquely over the ridge, cyclonic vorticity is produced as it flows from deeper to shallower water, and anticyclonic vorticity is produced as it moves from shallower water back into deeper water. Thus a symmetrical sign change in vorticity should be evident across the ridge.

IV. Methods, Observations and Preliminary Results

Moored Time Series Tidal Analysis

In order to fully understand the small-scale processes at work in an area known to be dominated by tides (Smith 1969), our first goal was to resolve the tidal structure in the sound. A mooring called N4 was deployed by Dick Limeburner in Vineyard Sound at 41°28.872' N latitude and 70°40.254' W longitude, to the northwest of Middle Ground (Figure 6). The mooring was outfitted with an RDI 300 kHz Acoustic Doppler Current Profiler (ADCP). This ADCP generated a time series of water velocity data over the entire water column, spanning the time period of August 17, 2006 to November 19, 2006. As expected, the time series reveals an ebb-

dominant tidal structure. The depth-averaged water velocity time series from the mooring is shown in Figure 7.
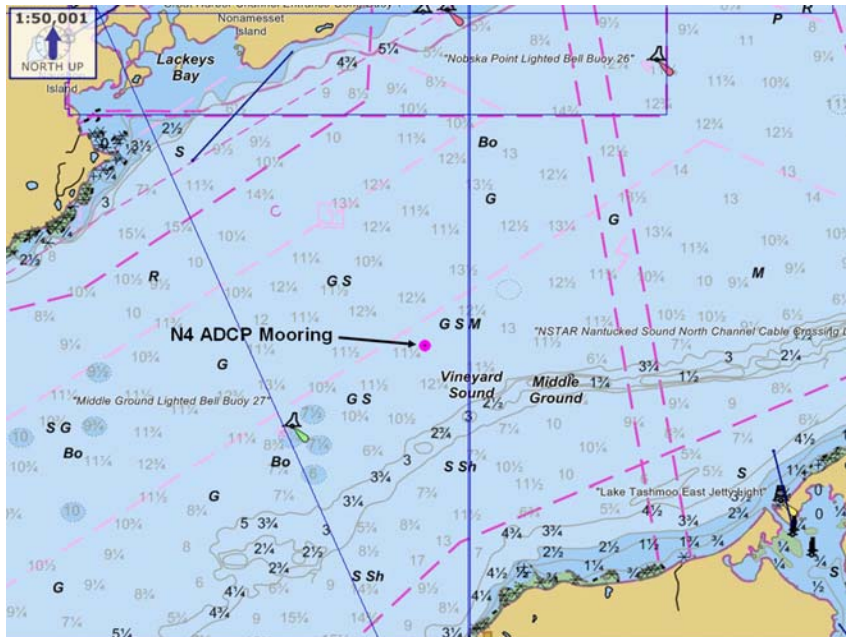

Figure 6: Location of N4 mooring in Vineyard Sound and relative to Middle Ground
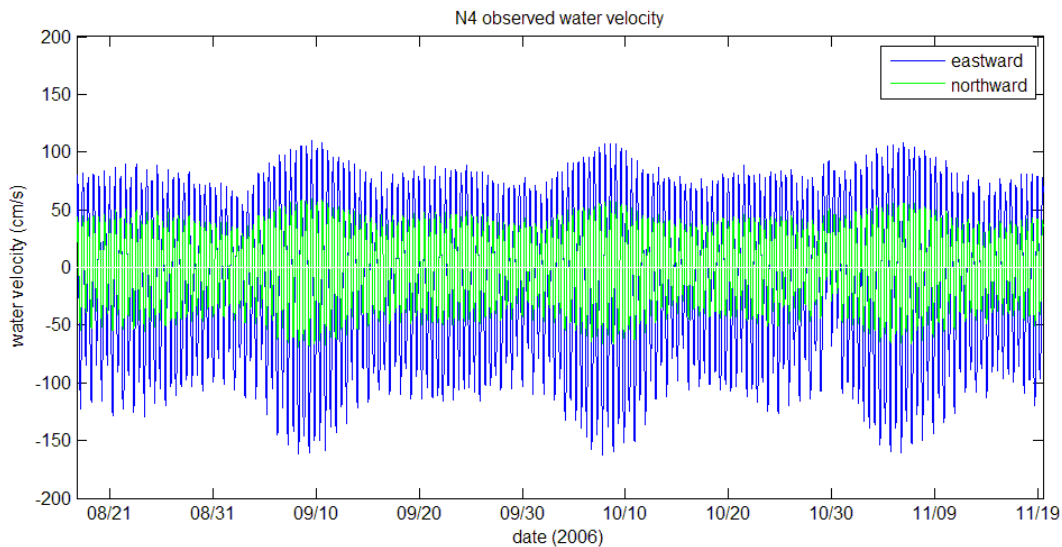

Figure 7: Depth-averaged water velocity time series produced by N4 ADCP. Notice what appears to be a strong weather event just before the third spring cycle.

We performed harmonic analysis on the entire N4 time series using the Matlab program t_tide (Pawlowicz et al. 2002). The program uses Fourier analysis to decompose the sinusoidal time series into a finite set of sinusoids at specific frequencies. These sinusoids represent the possible tidal constituents that interact to form the observed tide. The degree to which each constituent potentially contributes to the tide is determined by its amplitude as well as its signal-to-noise ratio (SNR). In Matlab, we pre-processed the raw time series by averaging both the east-west (u)

and north-south (v) velocity components over the entire water column, as shown in Figure 7. We then entered these depth-averaged velocity components into t_tide, along with the starting date and time of the time series and the latitude of the mooring. We sorted this data by the SNR of each constituent, and determined those constituents with and SNR over 20 to be the principal components of the observed tide. These constituents were also the only constituents with amplitude values over 2 cm, with the next largest amplitude value around 0.6 cm. Table I shows information generated by t_tide on the eight principal constituents.

Tide	Frequency (s^-1)	Major axis (cm)	Minor axis (cm)	Inclination (deg)
*M2	0.0805114	111.676	0.461	25.22
*N2	0.0789992	26.438	-0.017	25.1
*S2	0.0833333	19.994	-0.059	25.05
*K1	0.0417807	9.182	-0.181	24.37
*O1	0.0387307	6.495	-0.353	23.47
*L2	0.0820236	15.202	0.041	24.83
*M4	0.1610228	6.23	-0.066	16.21
*M6	0.2415342	4.937	0.486	25.88

Tide	Phase (deg)	Shift from M2 (deg)	Amplitude (cm)	SNR
*M2	26.78	0	55.83847575	7.70E+03
*N2	349.09	322.31	13.21900273	3.60E+02
*S2	43.2	16.42	9.997043525	2.30E+02
*K1	98.14	71.36	4.591891903	1.00E+02
*O1	74.23	47.45	3.252292807	57
*L2	100.42	73.64	7.601027644	48
*M4	295.97	269.19	3.115174794	45
*M6	315.53	288.75	2.480431666	25

Table I: Information generated from t_tide output for the 8 principal constituents of the N4 observed tide.

By comparing the major and minor axes for each constituent, we determined that the tide observed by the N4 mooring is extremely rectilinear (Figure 8). The orientation of the composite tidal ellipse is approximately 25 degrees north of east, or roughly oriented along the channel of Vineyard Sound. We then recreated the composite tide by calculating the sum of each of the eight principal sinusoids. As the N4 mooring was located on the north side of Middle Ground, we expected the tide to be ebb-dominant. This was indeed the case for the calculated composite tide (Figure 9).
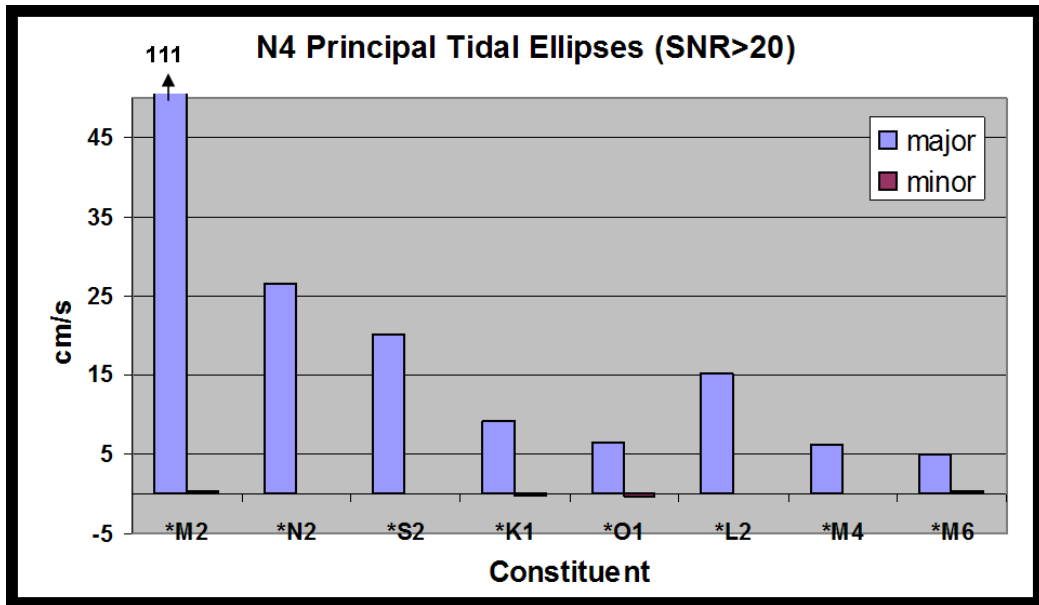
Figure 8: The strong dominance of the major axis in each principal constituent shows the observed tide to be highly rectilinear. The M2 major axis amplitude was 111.7 cm; it is truncated here to show the remaining constituents more clearly.
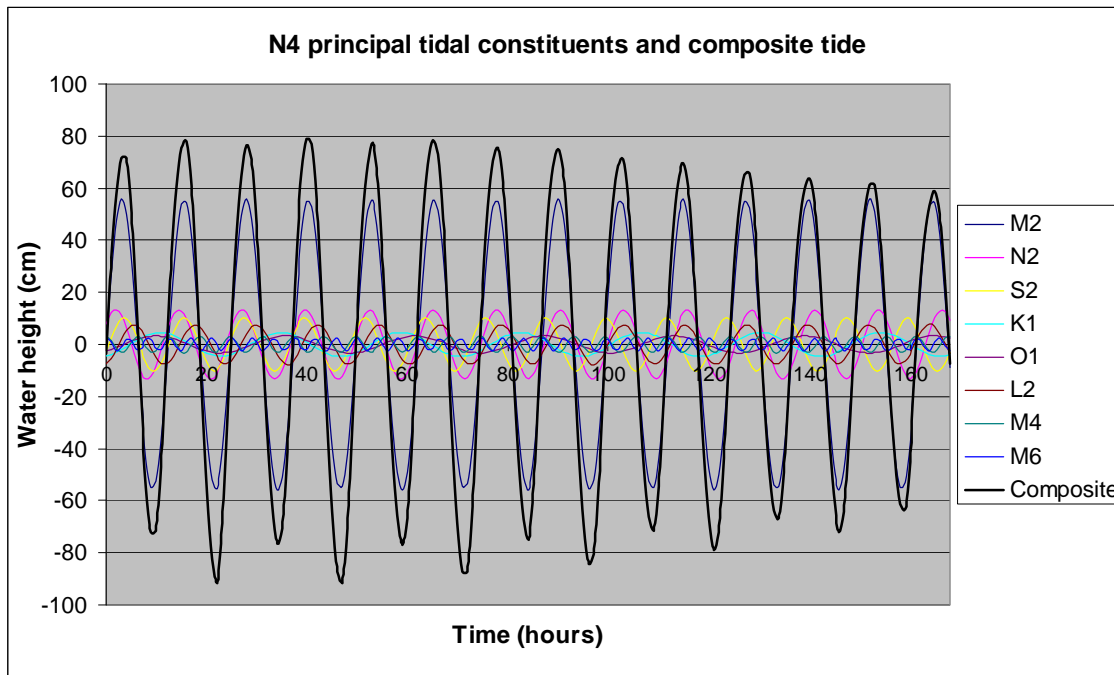

Figure 9: The largest tides shown over these recreated composite tidal cycles are ebb tides, which is consistent with the observations acquired by the N4 ADCP.

We isolated the flow from N4 in the direction of the major axis of the M2 tidal ellipse. We then ran this flow through a low frequency filter in Matlab to compare the energy of the low frequency flow to the envelope of the tide. This method was based on a similar method described by Signell (1987). As shown in Figure 10, a relationship may exist between the spring-neap cycle at N4 and the low frequency flow. During each spring cycle, a small increase

in southwestward flow is evident in the low frequency flow. This is difficult to resolve from the N4 time series alone, as a large weather event occurs immediately prior to the third spring tide. In order to fully resolve this relationship, a longer time series is necessary, as well as the removal of environmental forcing factors that may affect the overall flow in the sound, such as wind.
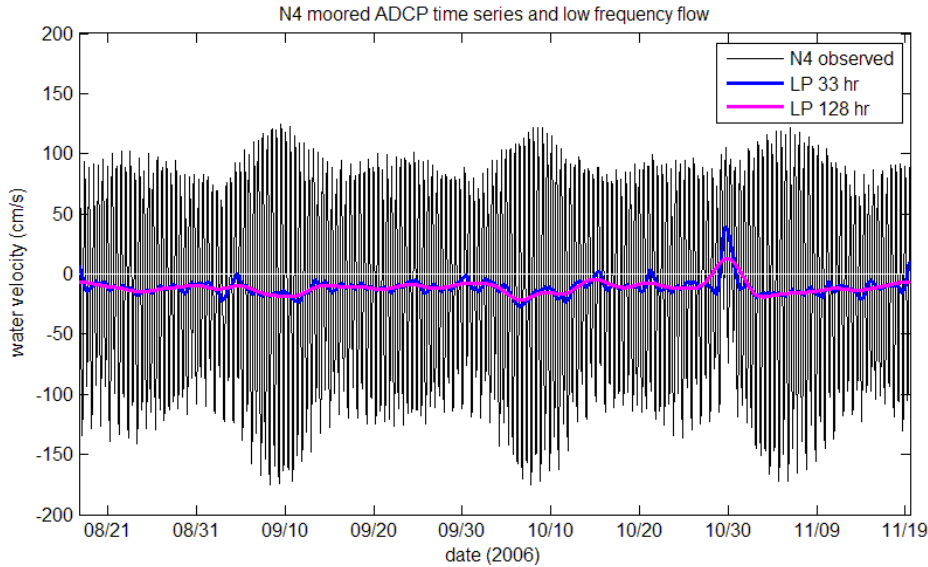

Figure 10: N4 velocity component in the direction of the M2 tidal ellipse and low frequency flow.

We computed the mean flow as well as the cube of the time series, or u^3. The latter is used as an indicator for sediment transport and thus has important implications for the maintenance of Middle Ground. Results are shown in Figure 11. The time series reveals a mean flow of magnitude 5-10 cm roughly in the direction of the ebb tide. The u^3 vector shows a strong component of turning towards the ridge. This turning could represent one half (i.e. the northern component) of a convergence of sediment onto the ridge.
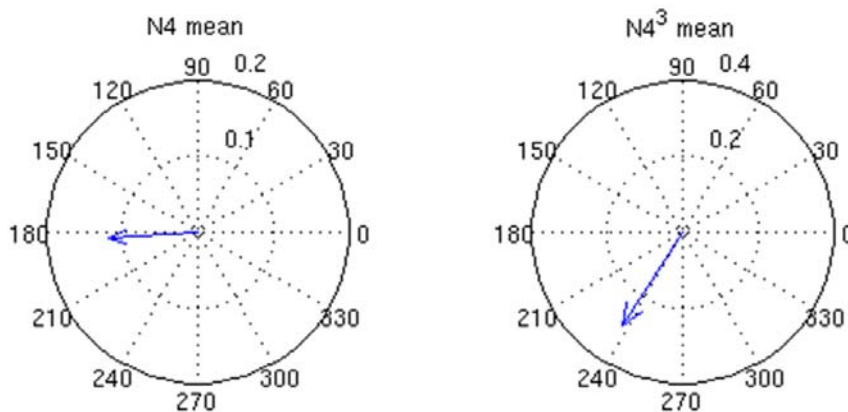

Figure 11: Mean flow and u^3 from N4 time series. Units are meters and m^3/s^3, respectively.

N4 Comparison to ROMS

We extracted a one-month time series from ROMS overlapping in time with the N4 time series. We compared the depth-averaged eastward component of velocity from ROMS and N4. Figure 12 shows that ROMS provides a good approximation of the tide at N4. However, the model consistently underestimates the relative amplitude of the ebb tide. Thus it may underestimate the discussed tidal asymmetry relative to the ridge. Again, this may have important implications for the small-scale processes we are attempting to resolve on and around Middle Ground.
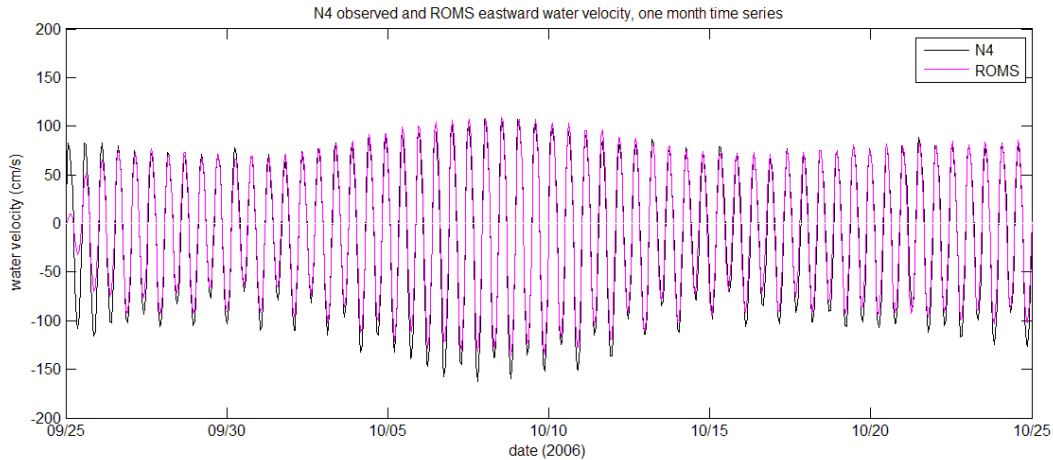
Figure 12: One month comparison of N4 and ROMS time series. Notice how ROMS consistently underestimates the dominance of the ebb tide.

One immediate result of this underestimation is that the mean flow and u^3 vectors from the ROMS time series are approximately half the magnitude of those from the N4 time series (Figure 13). Thus, if ridge shaping and maintenance relies on a convergence of sediment from all sides, the model may underestimate sand accumulation on the ridge. However, ROMS confirms the direction of these vectors calculated from the N4 time series. The mean flow is in the approximate direction of the ebb tide, and the u^3 vector has a strong component towards the ridge.
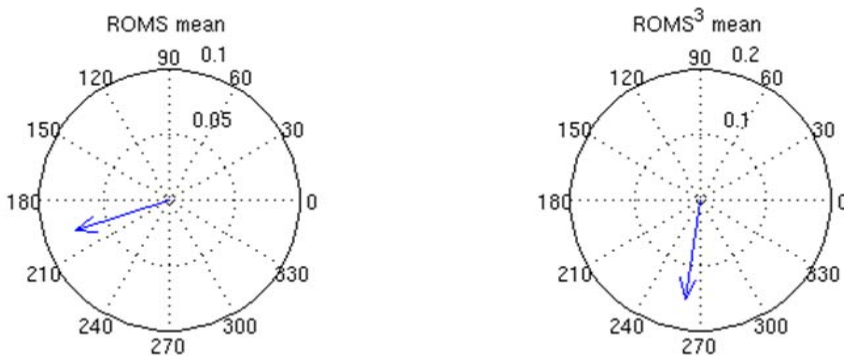

Figure 13: Mean flow and u^3 from ROMS time series. Units are meters and m^3/s^3, respectively.

REMUS Spatial Transects

In order to extend the *in situ* observations to locations closer to the ridge, we undertook a series of transects across it. Our primary goal was to obtain water column velocity data over the complete tidal cycle. A map of these transects is shown in Figure 14. The difference in location between the 2006 and 2007 transects is due to the change in bathymetry used to design them. In 2006, standard NOAA nautical charts were used. In 2007, high resolution bathymetry from the three USGS swath bathymetry surveys allowed more accurate planning of a transect running nearly normal to the main axis of the ridge.
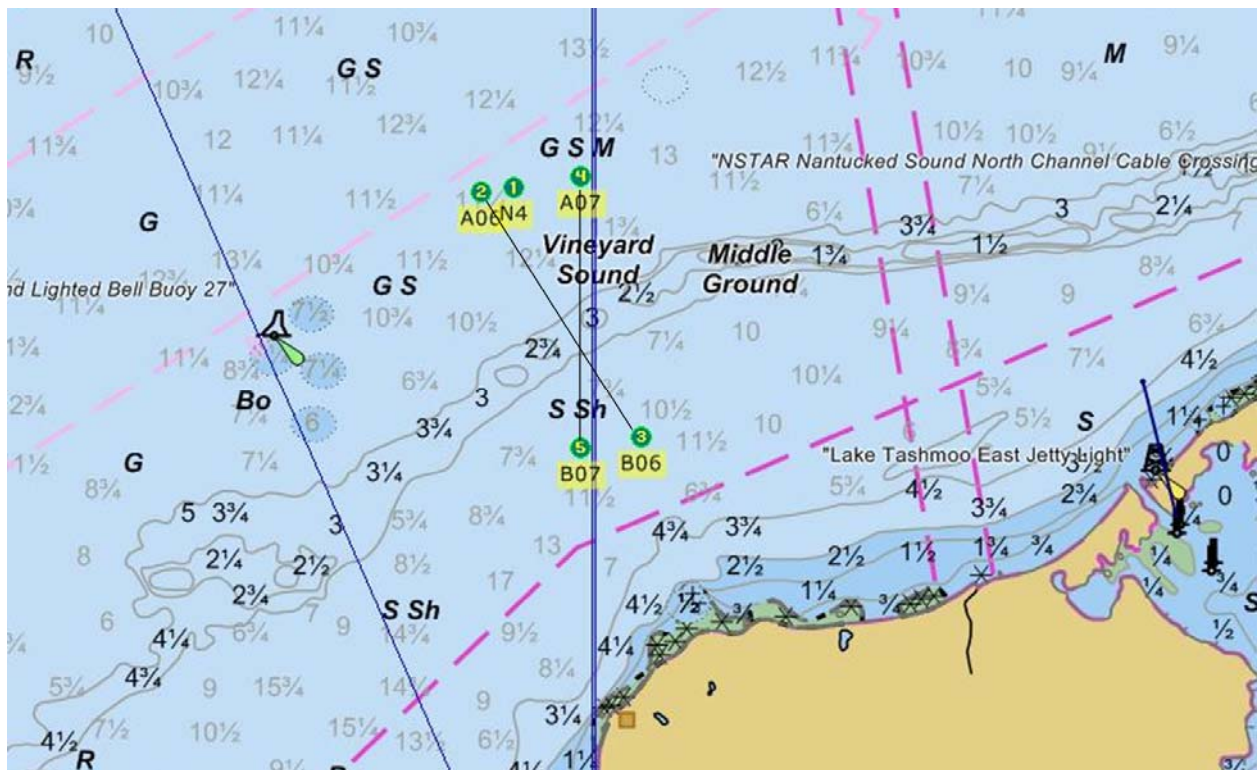

Figure 14: 2006 transect runs from waypoints 2 to 3. 2007 transect runs from waypoints 4 to 5. Waypoint 1 shows the relative location of the mooring N4. Notice the relative position of Middle Ground according to this NOAA nautical chart.

We used the Autonomous Underwater Vehicle (AUV) REMUS to complete the transects. The vehicle is equipped with both an up- and down-looking ADCP (Figures 15 and 16). Missions with REMUS were planned according to the tidal cycle in Vineyard Sound. Each set of REMUS missions was designed to capture one half of the tidal cycle, either ebb or flood. Over this cycle, our goal was to obtain cross-ridge transects at one- to one and a half-hour intervals, resulting in four to five missions for each half-cycle. The complete mission plan for the 2007 ebb tide is shown in Figure 17. The cross-ridge transect runs from waypoints A to B.
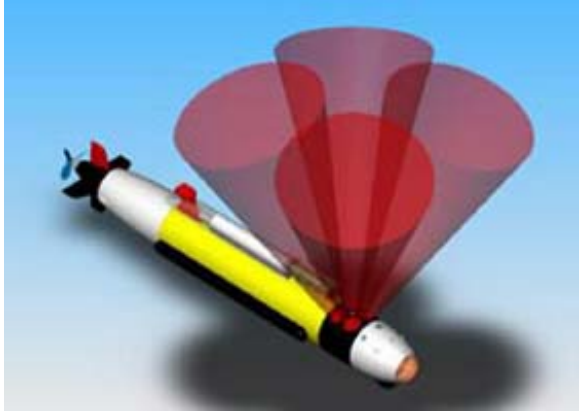
Figure 15: Diagram showing a REMUS vehicle and an exaggeration of the up-looking ADCP. Courtesy of NOAA.

Figure 16: Picture of the REMUS vehicle and interfacing laptop in the Ocean Systems Laboratory, WHOI.
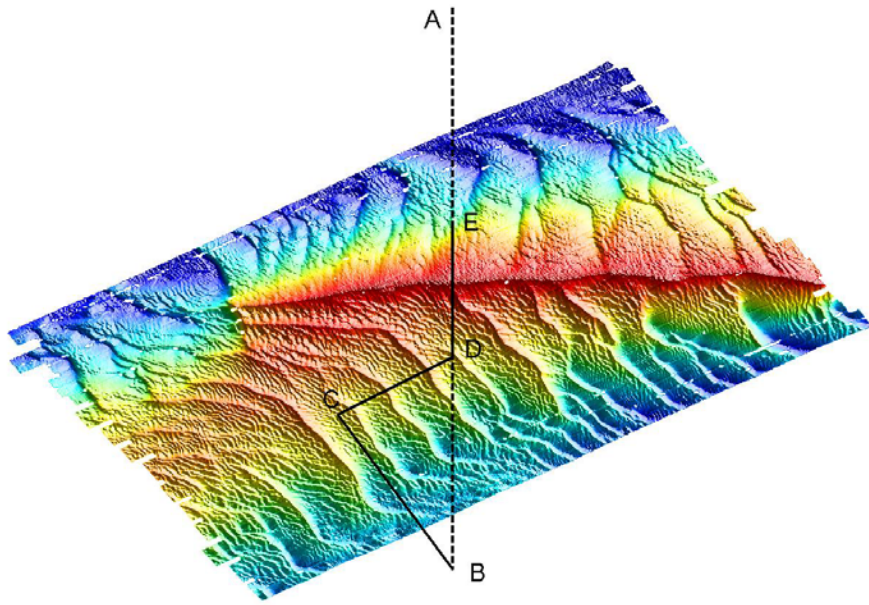
Figure 17: Mission plan for 2007 ebb cycle. Cross-ridge transect runs from waypoints A to B; slow cross-wave leg runs from waypoints C to D.

For this project, we used the down-looking ADCP exclusively. For the cross-ridge leg the vehicle flew at a constant speed of 3.5 knots and a constant depth of 2 meters, and the ADCP was set to a constant ping rate of one second. Each complete mission took approximately 40 minutes to complete, with the actual cross-ridge component taking 12-15 minutes. In between missions, the vehicle had to be recovered, and the mission data downloaded onto an interfacing laptop. The vehicle was then transported and redeployed at the starting waypoint.

The 2007 missions were also designed to include a "slow leg" (shown in Figure 17 from waypoints C to D). Here the vehicle flew at a slower speed directly against the tidal current. The goal of this leg was to collect data at a higher spatial resolution in order to investigate the velocity structure associated with sand wave ridges and crests. Due to technical difficulties with the vehicle this data was inconsistent. Thus this report will focus entirely on the cross-ridge transect data.

Raw ADCP data from REMUS was exported into Matlab using a combination of VIP, the REMUS interface software, and WinADCP software. An example of raw water velocity data from one depth bin is shown in Figure 18. Using pitch, roll, heading and bottom track velocity information recorded by the vehicle, this data had to be rotated from ship coordinates to earth coordinates. As the strongest currents in Vineyard Sound do not exceed 200 cm/s, this was used as the upper and lower definition for good data points. Velocity values outside of this range were culled. Bottom depth information recorded by the vehicle was then used to remove velocity values from bins below the physical bottom. Due to beam angle interference, only the top 85% of the ADCP profile was used. These final good data points were then averaged over the water column and binned to 20 second temporal resolution. This corresponds to a spatial resolution of approximately 36 meters per bin. An example of processed data is shown in Figure 19.
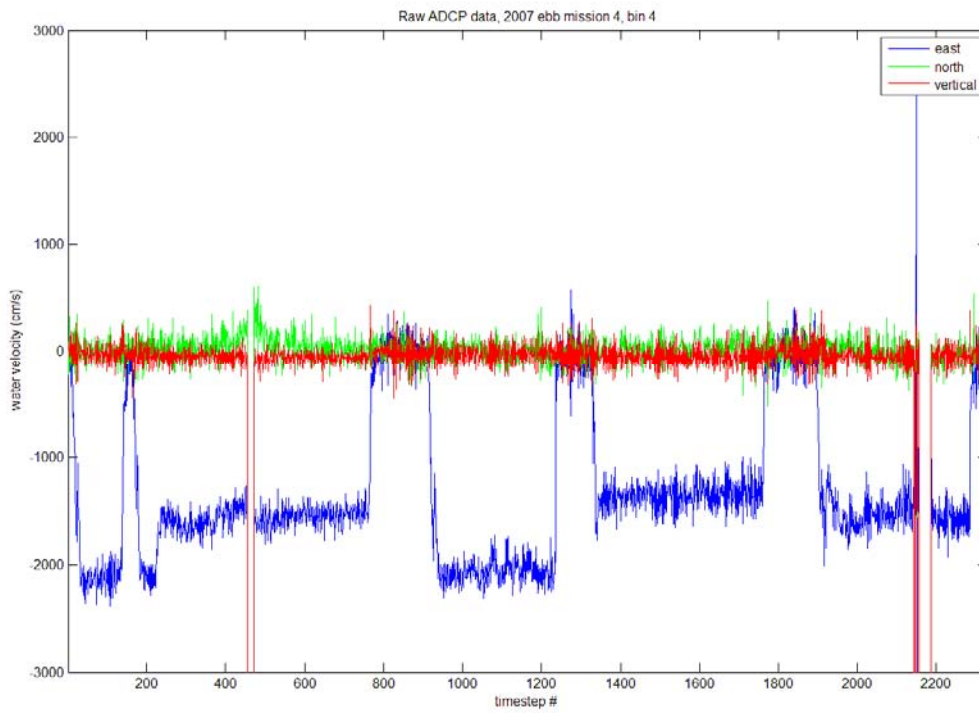
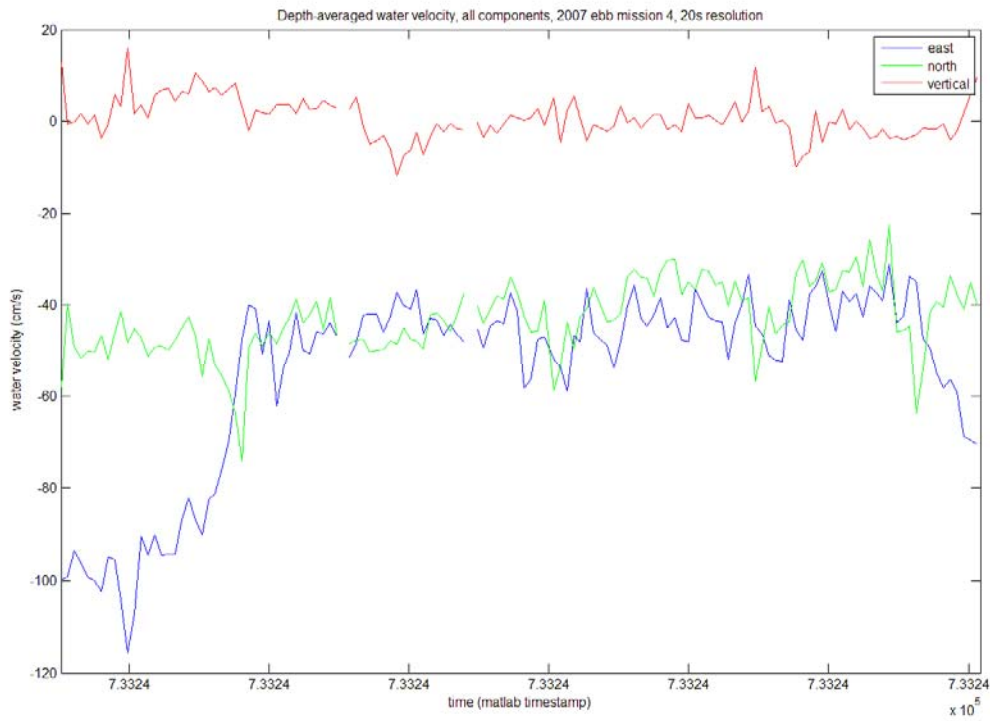**Figure 18: Unprocessed data from REMUS ADCP, 2007 ebb mission 4, depth bin 4.**

Figure 19: Processed data from REMUS ADCP, 2007 ebb mission 4, 20 second resolution.
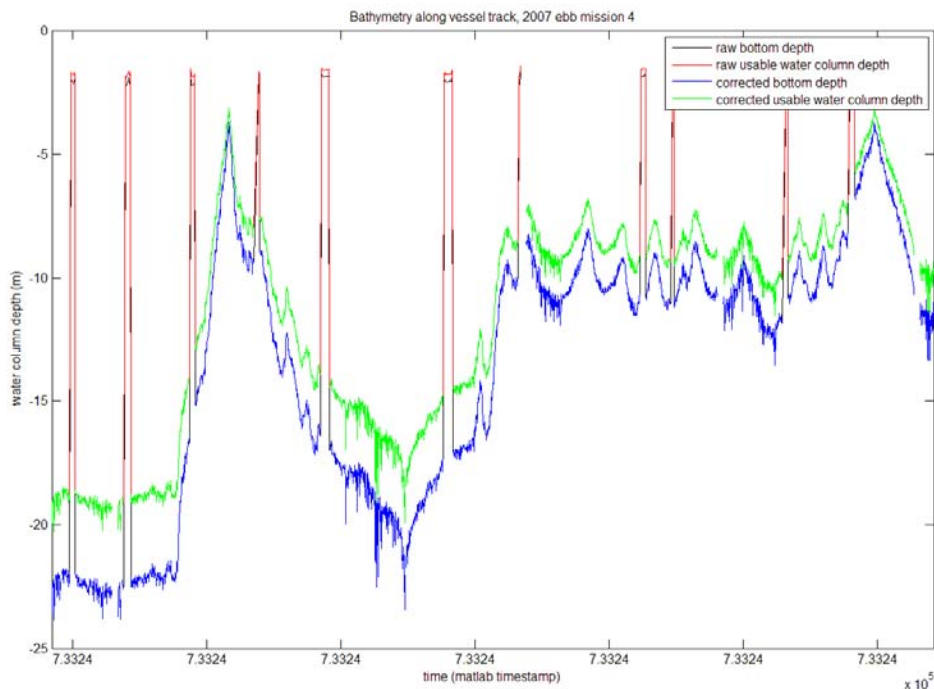
Figure 20: Bottom depth against time for the complete 2007 ebb mission 4. From this plot we can see that the vehicle traveled over the ridge, then over a set of sand waves, and finally back over the ridge crest. In the legend, "usable" denotes the top 85% of the water column as discussed.

The bathymetric information collected by the vehicle (as shown in the above figure) was used to isolate the cross-ridge transect for each mission. Processed water velocity data from this transect was plotted as a series of vectors along the vessel track (Figures 21 and 22). The direction of each vector relative to the transect line represents current direction in that location; the size of the vector represents the magnitude of that current.
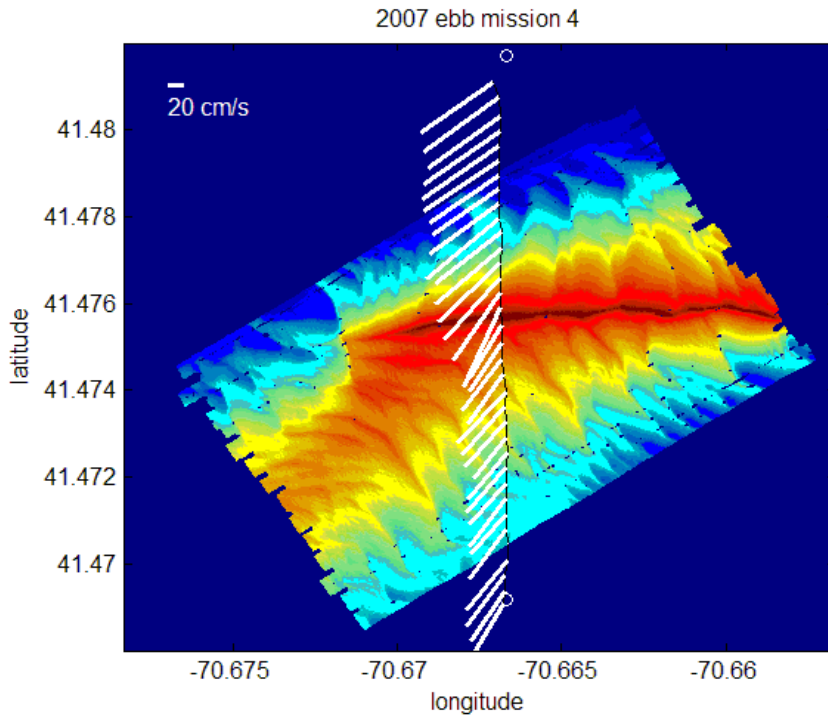
Figure 21: Plot of depth-averaged velocity vectors along vehicle track for 2007 ebb mission 4. Notice the strong shearing to the south of the currents directly over the ridge crest.
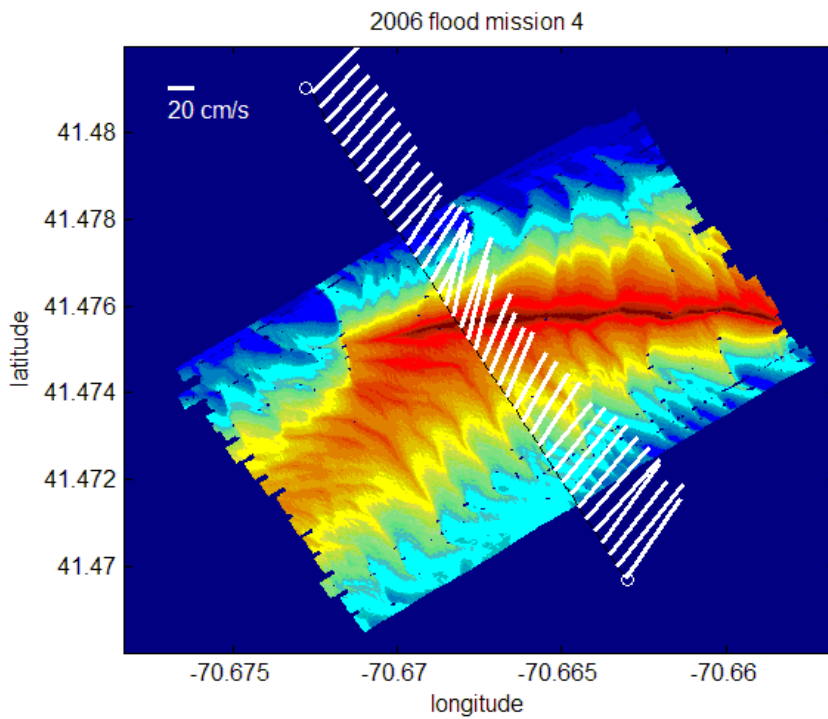

Figure 22: Plot of depth-averaged velocity vectors along vehicle track for 2006 flood mission 4. Notice the strong shearing to the north of the currents directly over the ridge crest.

These plots confirm the orientation of Middle Ground as oblique to the tidal flow. They also confirm the orientation of the principal tidal ellipse as observed by the N4 mooring. Plots from all of the REMUS transects acquired show strong evidence of shearing of the current directly over the ridge crest. The flow direction recovers from this shear almost immediately on the other side of the ridge. The magnitude of the flow, however, does not appear to recover entirely. The two transects shown in the above figures are representative of all REMUS transects obtained.

REMUS Comparison to ROMS

Overall, we collected 9 transects: 4 from a flood tide on September 25, 2006, and 5 from an ebb tide on July 13, 2007. We performed a point-to-point comparison between ROMS and REMUS velocities over the tidal cycle collected by REMUS. Point A is the northern endpoint of the 2007 REMUS cross-ridge transect, as shown in Figure 17. Point B is the southern endpoint of the same transect. ROMS tidal current information was extracted at those two points for the flood and ebb tide measured by REMUS. Three representative REMUS velocity vectors were averaged to approximately 120 meter resolution near points A and B, and those average velocities were compared to ROMS velocities. Comparison over the entire flood cycle is shown in Figure 23; comparison over the entire ebb cycle is shown in Figure 24. For the purpose of this particular comparison, only the eastward, or u component of the velocity is shown. The northward, or v component in the channel is much smaller and displays the same trends as the u component.
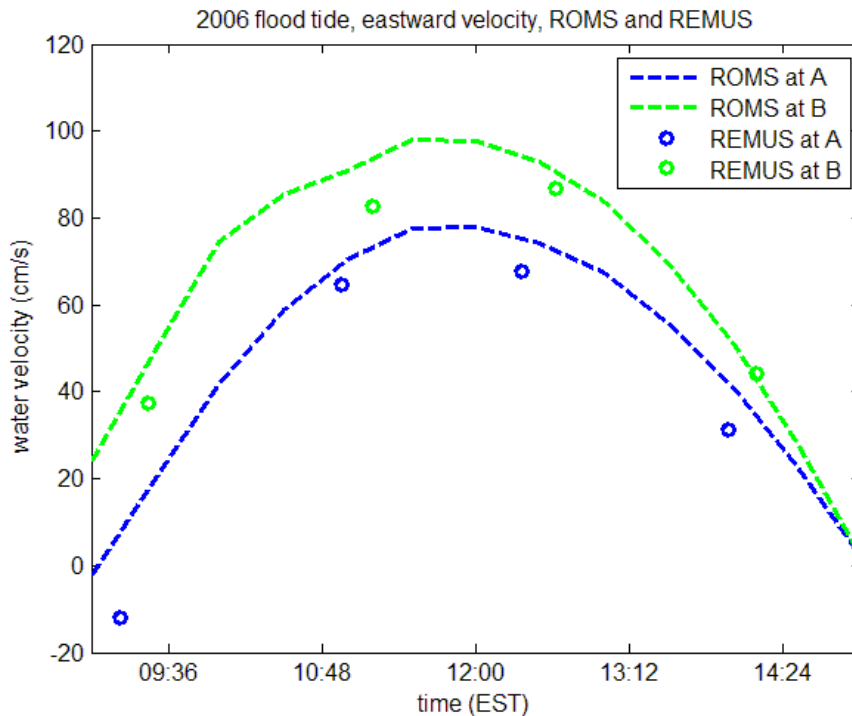

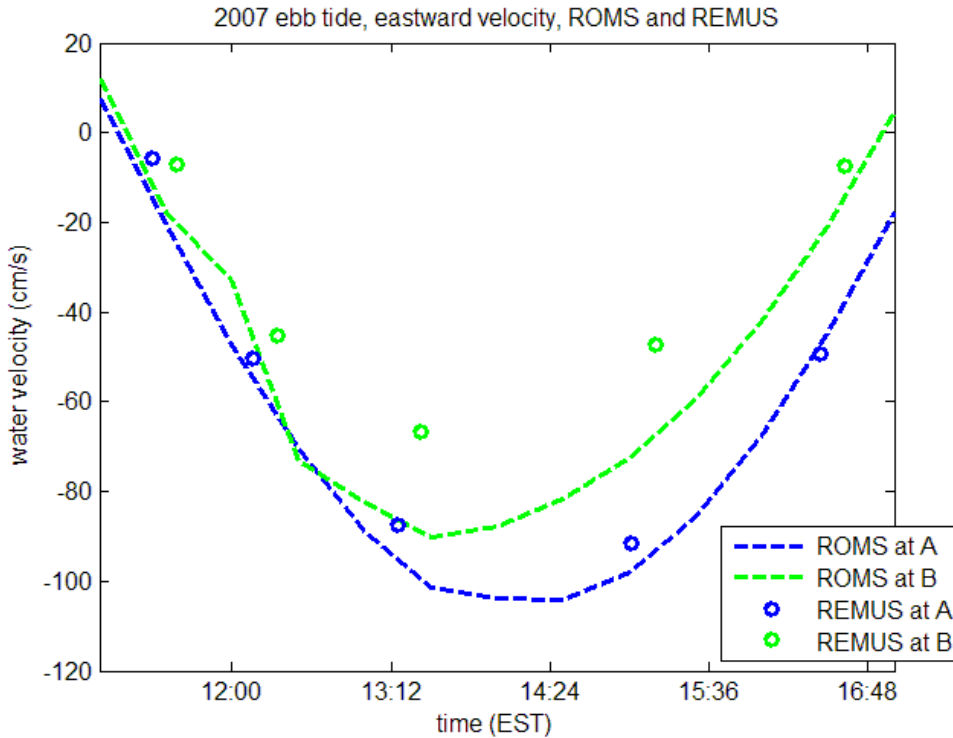**Figure 23: ROMS to REMUS comparison over entire flood cycle, 25 September 2006.**

Figure 24: ROMS to REMUS comparison over entire ebb cycle, 13 July 2007.

According to these figures, the transects acquired with REMUS are fairly evenly spaced and cover a broad range of phases in each half-cycle. Also, this comparison shows that ROMS provides an accurate approximation of the tidal cycle at points A and B. However, we also observe that the relationship between the moored ADCP at N4 and ROMS does not hold true for the data collected by REMUS. At N4, ROMS consistently underestimated the relative amplitude of the ebb tide. At A and B, ROMS is actually overestimating the amplitude of both the ebb and flood tides to a small degree. We see from the REMUS data that during the flood tide, the flow is stronger on the south side of the ridge. During the ebb tide, where the discrepancy between ROMS and REMUS is more significant, the flow is stronger on the north side of the ridge. This is consistent with the tidal asymmetry relative to the ridge previously discussed. Thus, although ROMS here overestimates the ebb tide, the flood/ebb asymmetry expected and observed at N4 may hold true at points A and B.

One other trend we notice from a comparison over the entire tidal cycle is as follows. For both the flood and ebb tides, at first slack water ROMS overestimates the REMUS velocities. As the tidal cycle progresses, the difference between the two data sets shrinks, until at or just after peak current, ROMS "catches up" to the REMUS data. After this point, ROMS begins to underestimate the REMUS data. A possible explanation for this trend is a small phase difference between ROMS and the real tide at points A and B. A ROMS predicted phase that is slightly behind that of the real tide would result in a trend like the one we observe.

We created vector plots along the vehicle track from ROMS data extracted along the entire transect. Figures 25 and 26 show these plots for comparison to the REMUS missions shown in Figures 21 and 22. The sharp shearing of currents directly over the ridge seen in the REMUS

vector plots is not evident in the ROMS plots. However, similar to observations from the REMUS plots, a loss of energy of the flow is evident after the flow crosses the ridge. The dramatic difference between the bathymetry used in ROMS and that from the high-resolution USGS survey is also evident in these plots.
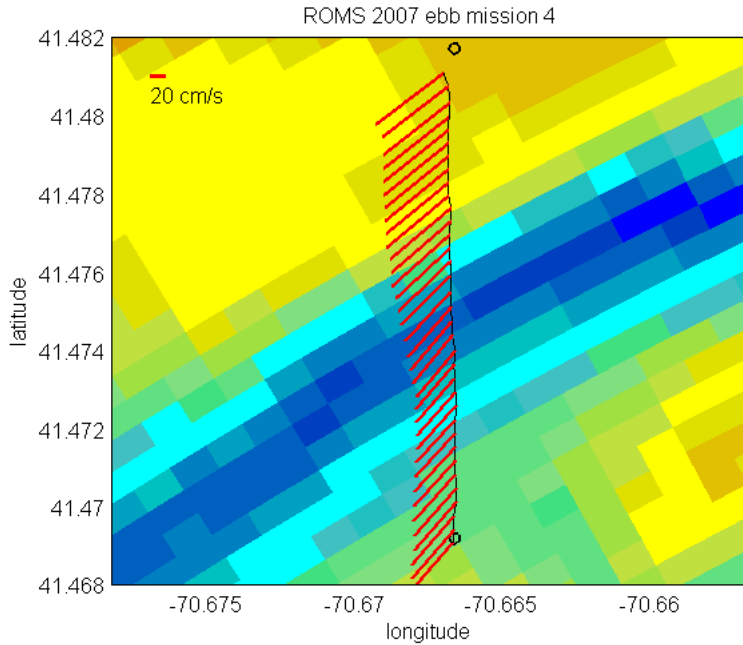

Figure 25: Depth-averaged velocity vectors from ROMS along REMUS track, 2007 ebb mission 4. Notice the apparent lack of shear as the flow crosses the ridge.
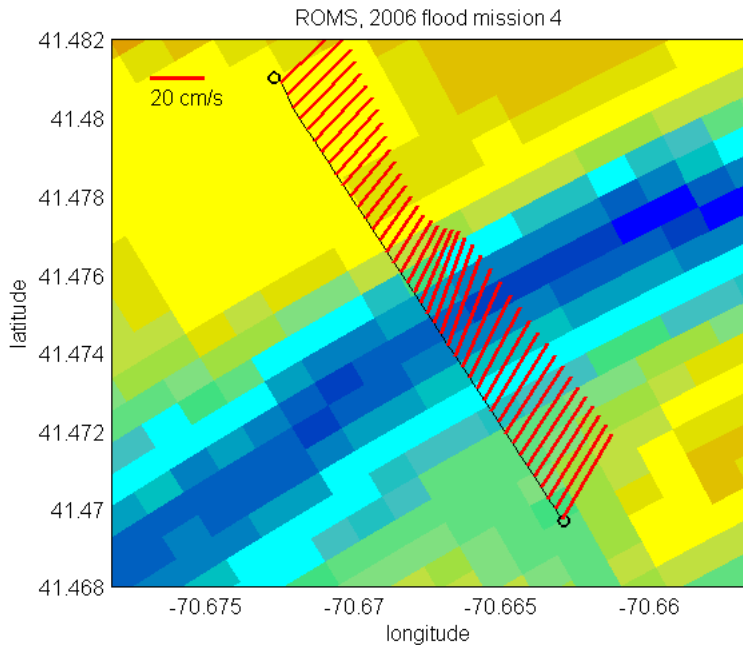

Figure 26: Depth-averaged velocity vectors from ROMS along REMUS track, 2006 flood mission 4.

Figure 27 shows a comparison of ROMS and REMUS u- and v-component velocities along the cross-ridge transects obtained near slack water and peak currents for the flood tide. Each velocity comparison overlays a profile of bottom topography from ROMS and REMUS along the transect.
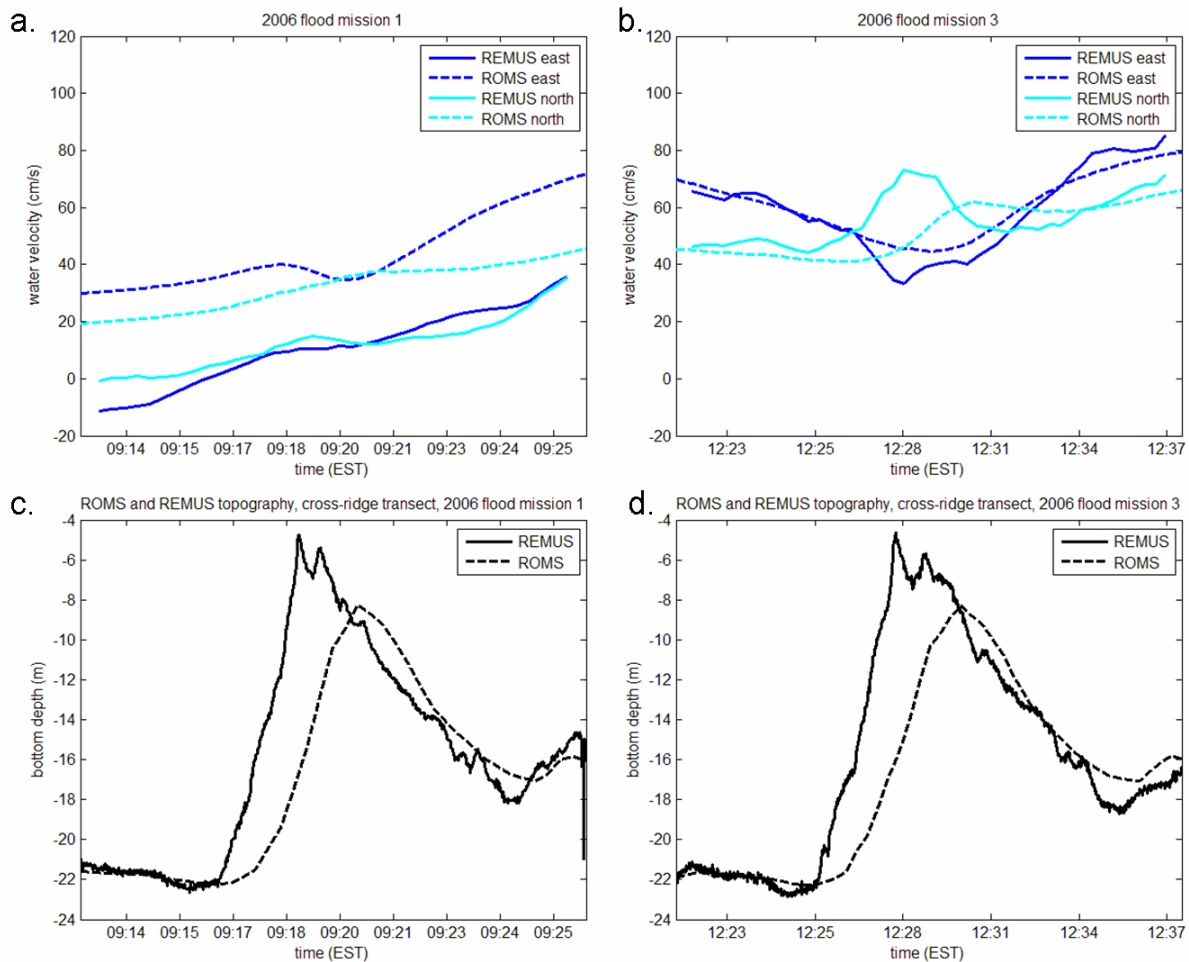

Figure 27: ROMS and REMUS cross-ridge velocities and topography for 2006 flood missions 1 and 3, near slack water and peak currents, respectively. Each plot of velocity overlies its corresponding bottom topography (a and c, b and d).

From these comparisons we see that the influence of the ridge on the flow is much more apparent when the currents are at a maximum than when they are at a minimum. A possible explanation for this is that as the current increases in magnitude, the frictional force caused by interaction with the bottom increases and thus has a stronger effect on the flow. We also observe that the disagreement between ROMS and REMUS velocity values are larger during slack water than they are around the peak of the tide. This is consistent with the trend discussed following Figures 23 and 24. Overall, ROMS again appears to predict currents in this region accurately. During mission 3 (peak currents), the sharp increase in northward velocity, simultaneous with a decrease in eastward velocity, are underestimated by ROMS. The time lag between ROMS and REMUS data for these sharp changes, however, can be accounted for by the difference in bathymetry shown in the bottom half of each figure. Middle Ground shifted northward at this

point significantly from its location on the NOAA charts. As a result, the large-scale changes in velocity seen in the REMUS data along the cross-ridge transect are shifted accordingly in the ROMS data. However, as is evident in both the vector plot comparison and the comparison in Figure 27, those changes are highly localized to the ridge crest. Figure 28 shows the same comparison for the ebb tide, again near slack water and peak currents. The results are consistent with those from the flood tide, although the apparent shear over the ridge is smaller. Here we compare the second slack water transect (at the end of the ebb cycle) to a transect at near peak currents, whereas in Figure 27 we compare the first slack water transect. Whereas in Figure 27, ROMS overestimates the REMUS velocities near slack water, here ROMS underestimates them. This is consistent with the phase shift between ROMS and REMUS mentioned previously.
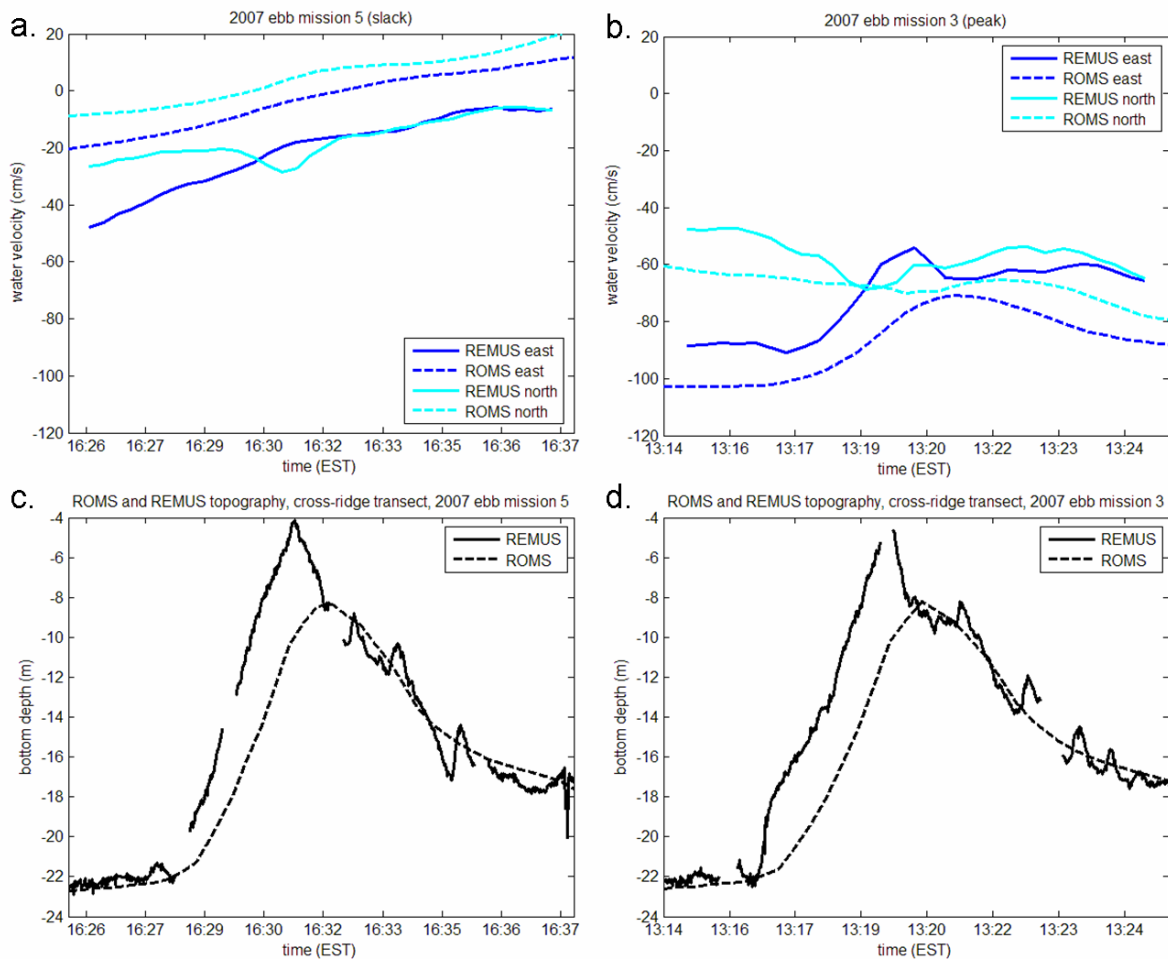

Figure 28: ROMS and REMUS cross-ridge velocities and topography for 2007 ebb missions 5 and 3, near slack water and peak currents, respectively. Each plot of velocity overlies its corresponding bottom topography (a and c, b and d).

Figures 29 and 30 show a comparison of shear of ROMS and REMUS velocities along the cross-ridge transects obtained near slack water and peak currents for the flood and ebb tides, respectively. These plots confirm the relative absence of shear during a period of minimal currents. They also confirm the relative timing (which in this case translates to distance across the ridge) between ROMS and REMUS for changes across the ridge. In this case, a sign change in shear is evident as the flow crosses the ridge. This sign change is confirmed by ROMS,

although the ROMS data is much smoother than the REMUS data. For all of these figures, REMUS velocity data has been smoothed to match the 100-120 meter resolution of ROMS. In the case of shear, the physically smoother bathymetry of the ROMS model may account for the discrepancy we see between the model and the field data.
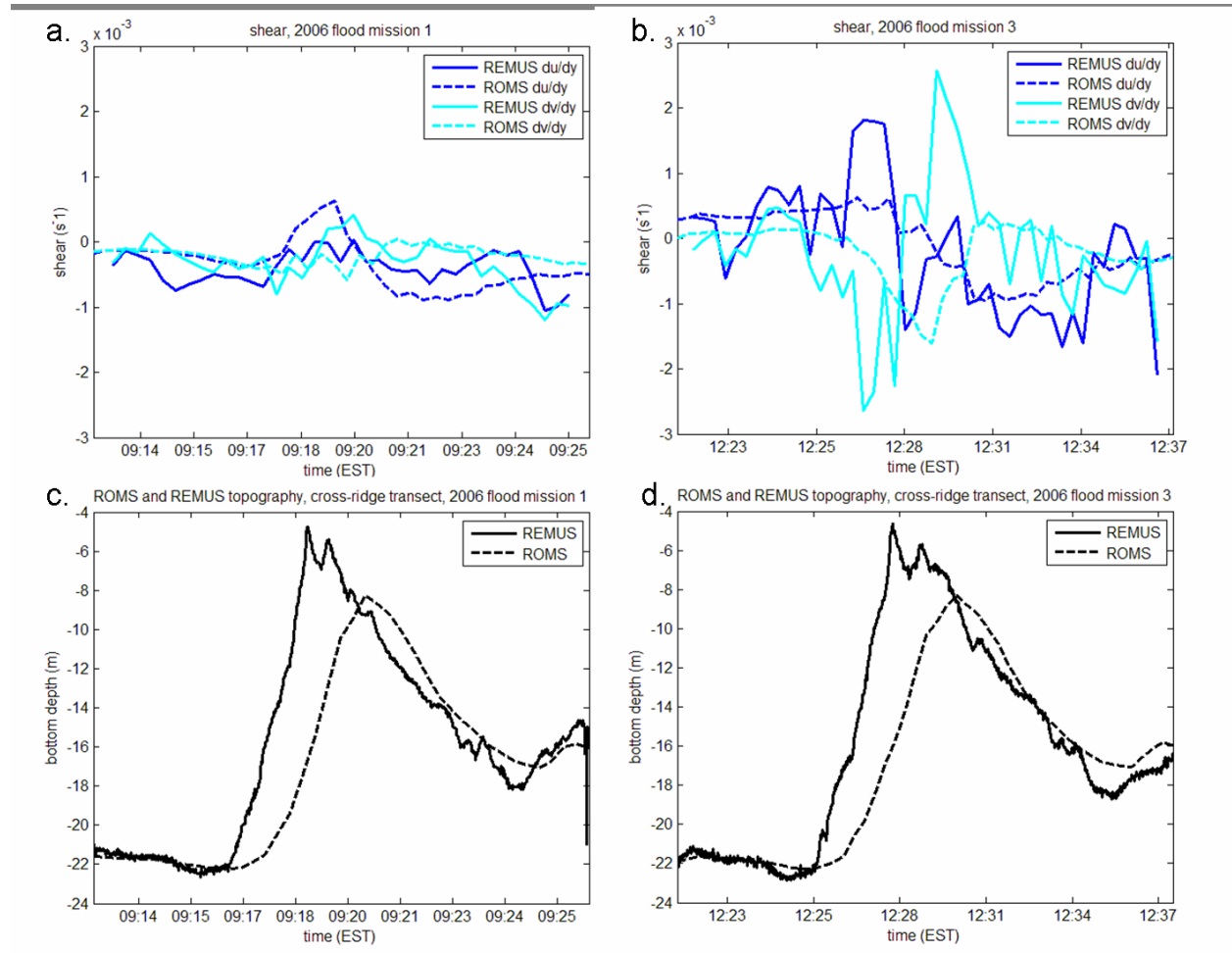

Figure 29: ROMS and REMUS shear in velocity along cross-ridge transect, 2006 flood missions 1 and 3, near slack water and peak currents, respectively.
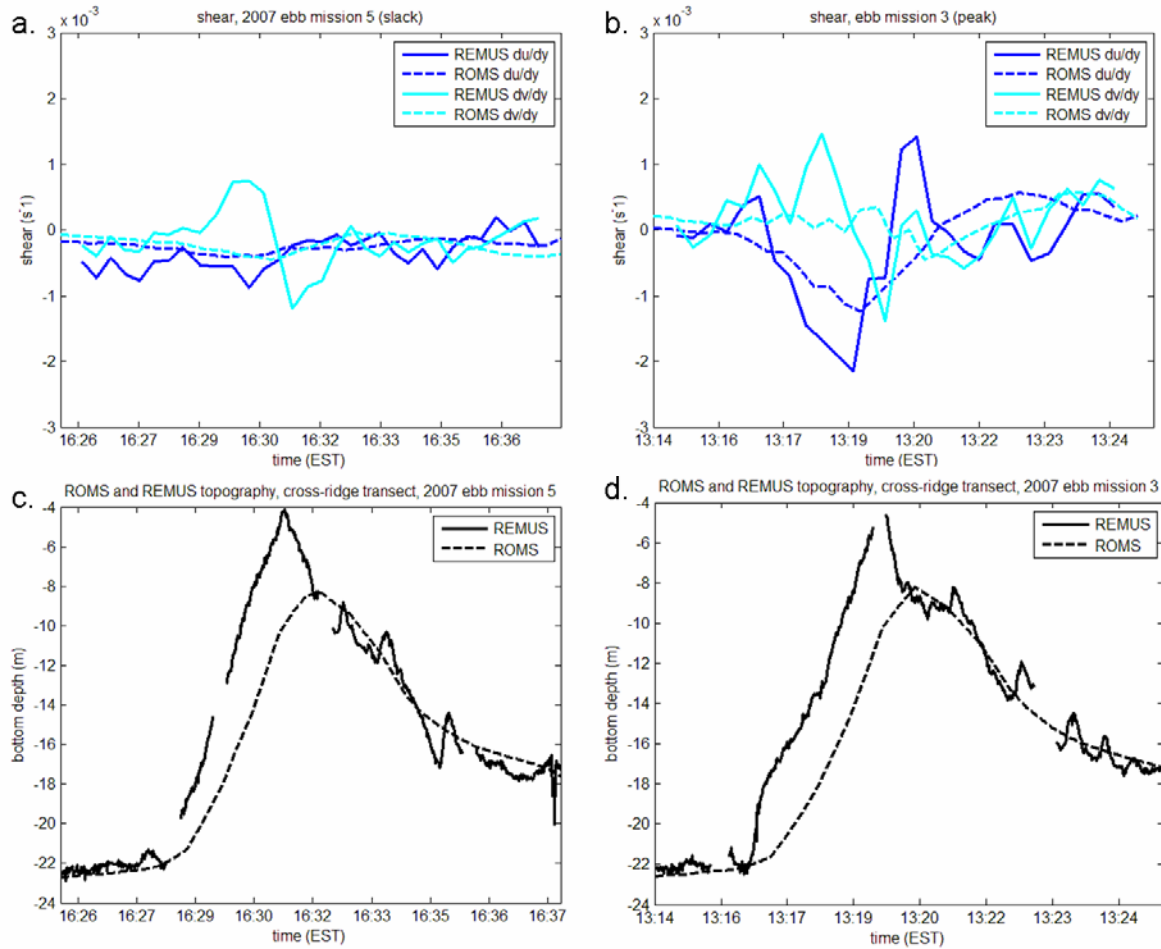
Figure 30: ROMS and REMUS shear in velocity along cross-ridge transect, 2007 ebb missions 5 and 3, near slack water and peak currents, respectively.

V. Preliminary Conclusions and Future Work

Based on the analysis of the N4 time series, there is a mean flow of 5-10 cm/s in the direction of the ebb tide. When we consider that ROMS underestimates the strength of the ebb tide, the comparison of N4 to ROMS over a one month time series confirms this mean flow. As tidal information and bathymetry are the only variables input into ROMS, we infer that this mean flow is tidally induced. In other words, rather than wind, pressure gradient, or other forces, the tidal flow within Vineyard Sound is primarily responsible for a mean flow of 5-10 cm/s towards the southwest. The observation that the u^3 vector has a strong component towards the ridge was also confirmed by ROMS. However, more evidence is necessary in order to draw conclusions about sediment transport in that direction. The u^3 vector at N4 represents only half of a convergence we expect to see of sediment towards the ridge. Another moored ADCP, N5, has been deployed on the south side of the ridge. Recovery of this mooring and analysis of the time series it generates are expected to provide the necessary evidence.

Based on the N4 comparison we also conclude that ROMS is an accurate tool for predicting tides on and around Middle Ground. However, the model may underestimate the tidal asymmetry observed at N4. If this tidal asymmetry is crucial to ridge maintenance (as it appears to be), the model may not provide the complete story of Middle Ground that is the objective of this project. In order to further investigate this discrepancy between ROMS and field data, it is important that the bathymetry in ROMS be updated to include the most current ridge position and parameters.

The REMUS spatial transects obtained so far are not consistent with the results from the N4 mooring, in that ROMS actually overestimates both the flood and ebb tide measured. Thus, it may be an oversimplification to state that the tidal asymmetry observed at N4 is characteristic of the entire region to the north of the ridge. In other words, there may be significant spatial variability in the tidal asymmetry relative to Middle Ground. In order to resolve this variability, spatial comparison to ROMS is necessary. Also, more REMUS transects need to be obtained throughout the tidal cycle, as well as at different points along the ridge.

Finally, we can conclude that there is a highly localized shear directly over the ridge during the strongest currents of both the flood and ebb tides. This shear is confirmed by ROMS, although the model underestimates the magnitude seen in the REMUS data.

These conclusions allow us to take a more informed look at the models of small-scale processes discussed earlier. Based on the shear data, we eliminate Robinson's model of vorticity. The sign change evident over the ridge in the REMUS data is not symmetrical with respect to the ridge. Also, Pingree's model of headland eddies appears to apply only conceptually to the original formation of Middle Ground. At the same time, our results thus far are consistent with both the tidal residual model and Huthnance's discussion of bottom friction. Both of these models indicate a mean flow to the southwest, with is confirmed by the N4 time series analysis. However, in order to fully relate these models to the Middle Ground system, it is necessary to obtain time series data closer to the ridge. Both models also call for further analysis on the south side of the ridge. For the tidal residual model, data from the south side could complete the picture of water and sediment convergence on the ridge. Data that revealed a mean flow to the northeast on the south side would further confirm the model of bottom friction. Thus, with more data we will be able to further resolve these small-scale processes and their role in the ridge system, and ultimately generate a complete story of Middle Ground.

Acknowledgments

References

Duffy, G. P. and Hughes-Clarke, J. E. "Application of spatial cross correlation to detection of migration of submarine sand dunes." Journal of Geophysical Research, Vol. 110 (2005).

Huthnance, J.M. "Tidal Current Asymmetries over the Norfolk Sandbanks." Estuarine and Coastal Marine Science I (1973): 89-99.

Knaapen, M.A.F. et al. "Quantifying bedform migration using multi-beam sonar." Geo-Mar Lett 25 (2005): 306-314.

Pawlowicz, R., B. Beardsley, and S. Lentz, "Classical Tidal Harmonic Analysis Including Error Estimates in MATLAB using T_TIDE." Computers and Geosciences, 28 (2002): 929-937.

Pingree, R. D. "The Formation of the Shambles and Other Banks by Tidal Stirring of the Seas." Journal of the Marine Biological Association of the U.K., 58 (1978): 211-226.

Robinson, I.S. "Chapter 7: Tidally Induced Residual Flows", Physical Oceanography of Coastal and Shelf Seas. Elsevier Oceanography Series, 35 (1983): 321-355.

Signell, R.P. "Tide- and Wind-forced Currents in Buzzards Bay, Massachussetts." Woods Hole Oceanographic Institution (1987): 51-60.

Signell, R.P. and Harris, C.K. "Modeling Sand Bank Formation Around Tidal Headlands." Estuarine and Coastal Modeling, (2000), 6th Int. Conf., ASCE, New Orleans, LA, November 3-5, 1999.

Smith, J. D. "Geomorphology of a Sand Ridge." University of Chicago, 1969.